

Comparison of critical and lowest-Landau-level scaling of the specific heat of several $\text{YBa}_2\text{Cu}_3\text{O}_{7-\delta}$ single crystals

Neil Overend, Mark A. Howson, and Ian D. Lawrie

Department of Physics, University of Leeds, Leeds LS2 9JT, United Kingdom

Stuart Abell and P. J. Hirst

National Crystal Growth Facility, Department of Materials Science, University of Birmingham, Birmingham B15 2TT, United Kingdom

Chen Changkang, Shamima Chowdhury, and John W. Hodby

National Crystal Growth Facility, Clarendon Laboratory, Parks Road, University of Oxford, Oxford OX1 3PU, United Kingdom

S. E. Inderhees and Myron B. Salamon

Department of Physics and Materials Research Laboratory, University of Illinois, West Green Street, Urbana, Illinois 61801

(Received 15 May 1995; revised manuscript received 11 April 1996)

The specific heat of two twinned and one detwinned single-crystal samples of $\text{YBa}_2\text{Cu}_3\text{O}_{7-\delta}$ have been measured with magnetic fields up to 8 T applied parallel to the c axes of the crystals. The crystals have zero-field transition widths of 0.3, 1.0, and 1.5 K. The zero-field data are analyzed in terms of the critical and Gaussian fluctuation models and the in-field data are analyzed in terms of critical and lowest-Landau-level (LLL) scaling. The data scale using the three-dimensional X - Y model in magnetic fields up to 8 T (the highest field we used). We also find LLL scaling to work, but only above 6 T. The implication is that there may be a crossover from three-dimensional XY to LLL scaling at some sample-dependent field of the order of 10 T. The results agree with recent measurements of the penetration depth and provide strong evidence for the existence of a critical regime within which there is scaling behavior characteristic of the three-dimensional X - Y model with critical exponents consistent with those observed in superfluid ^4He . We then perform the same analysis on previously published specific-heat data on $\text{YBa}_2\text{Cu}_3\text{O}_{7-\delta}$ and $\text{LuBa}_2\text{Cu}_3\text{O}_{7-\delta}$ in order to demonstrate the universality of the scaling functions. [S0163-1829(96)01738-9]

INTRODUCTION

A common characteristic of the high- T_c superconductors is the observation of significant effects due to thermodynamic fluctuations at temperatures near to the superconducting transition temperature T_c . In conventional superconductors fluctuation effects are generally small due to the large coherence lengths in these materials (see Ref. 1 for a review of fluctuation effects in conventional superconductors). As a result, mean-field theory provides an adequate description of observed physical properties. In the presence of a magnetic field, mean-field theory predicts that the transition temperature of a type-II superconductor is reduced and the phase diagram in the H - T plane contains two regions (superconducting and normal) separated by the temperature-dependent upper critical field [$H_{C2}(T)$] line.

It is well known that the specific heat of a conventional superconductor in zero magnetic field exhibits a discontinuity at T_c and this behavior is well described by mean-field theory without taking fluctuation effects into account. Roughly speaking the effect of fluctuations on the specific heat is to broaden the superconducting transition and smooth the sharp discontinuity at T_c although there is still a cusp at $T=T_c$. Whilst mean-field theory provides an excellent explanation of the specific heats of bulk samples (in zero-magnetic field) the specific heat of dirty (i.e., short coherence lengths), two-dimensional samples exhibit measurable effects due to thermodynamic fluctuations. In this case, the

broadening of the transition in zero magnetic field can be described by Gaussian corrections to mean-field theory.¹ In high-temperature superconductors, fluctuation effects are enhanced by the intrinsically very short coherence lengths and high transition temperatures characteristic of these materials. Close to T_c , fluctuations can then become so large that mean-field theory with Gaussian corrections no longer describes the observed behavior.² This provides an opportunity of observing critical fluctuations at a superconducting phase transition and determining the universality class to which this transition belongs. The temperature range over which the effect of critical fluctuations on the specific heat should be observed is not well known. The Ginzburg criterion is often used to estimate this temperature range, but this underestimates the true size of the critical region.³ Recent estimates suggest that the critical region of $\text{YBa}_2\text{Cu}_3\text{O}_{7-\delta}$ in zero field extends as much as 10 K above and below T_c .³ In particular, recent measurements of the penetration depth by Kamal *et al.*⁴ have shown that the penetration depth, $\lambda(T)$, is proportional to $(T-T_c)^{-1/3}$ over a temperature range of 10 K below T_c which is consistent with three-dimensional (3D) XY critical behavior.

The universality class of the superconducting transition is at present uncertain, but there is now growing evidence that $\text{YBa}_2\text{Cu}_3\text{O}_{7-\delta}$ exhibits critical fluctuations characteristic of the three-dimensional XY model.⁵ For an uncharged Bose fluid, such as liquid ^4He , we expect to observe 3D XY critical behavior with the exponent for the correlation length⁶

$\nu \sim 0.66$. The evidence is mounting that this is also the universality class for high- T_c superconductors within the experimentally accessible temperature range near T_c . Within a temperature range that is probably too small to be accessible, effects due to fluctuations in the vector potential, present because Cooper pairs carry charge, are expected. These have been predicted to lead to a first-order phase transition in $4-\epsilon$ dimensions⁷ but second order in $2+\epsilon$ dimensions.⁸ A numerical simulation in 3D suggests a second-order transition.⁹ But we emphasize that in an extreme type-II superconductor this region of fluctuations in the vector potential is probably experimentally inaccessible, and so we expect to observe critical behavior in a region around T_c governed by 3D XY critical exponents similar to the liquid ⁴He. In this region the general theory of scaling suggests that the singular part of the specific heat should be of the form $C_s = g_B^{-\alpha\phi} f(g_T/g_B^\phi)$ where the scaling fields g_B and g_T are the appropriate linear combinations of $T-T_c$ and B , and α and ϕ are the critical exponents. The scaling function $f(x)$ should have limits $f(0)=f_0$ and $f(x) \approx f_\infty x^{-\alpha}$ as $x \rightarrow \infty$, where f_0 and f_∞ are finite, nonzero constants, implying the existence of two scaling axes, $g_B=0$ and $g_T=0$, along which C_s has pure power-law behavior $C_s = f_\infty g_T^{-\alpha}$ or $C_s = f_0 g_B^{-\alpha\phi}$. In principle, the exponents α and ϕ and the scaling fields g_B and g_T can be identified from the renormalization-group eigenvalues and eigenvectors at the appropriate fixed point. However, the renormalization-group structure for a superconductor in a magnetic field is not known. From the symmetry of the phase diagram under the reversal of B , we can deduce that one scaling axis is $B=0$ and identify $g_B=B$. Then at $B=0$, $g_T \propto T-T_c$, while α is the exponent associated with the zero-field singularity. Assuming that B enters principally through a characteristic length scale $\approx B^{-1/2}$ (the Larmor radius), one expects $\phi=1/2\nu$, where ν is the correlation length exponent. Within the Hartree approximation,¹⁰ these expectations are verified, and the scaling field g_T can be identified as $g_T=T-T_c(B)$, where $T_c(B)$ corresponds to the upper critical field in mean-field theory. Theoretical estimates for the three-dimensional XY model⁶ give $\nu=0.669 \pm 0.002$, while the measured value¹² of ν in liquid ⁴He is 0.672 ± 0.001 .

The broadening of the superconducting transition in a magnetic field has recently been discussed in terms of the lowest Landau level (LLL) approximation,^{13,14} which applies in a region of the phase diagram close to the renormalized $B_{c2}(T)$ line, when the magnetic field is large enough for the paired quasiparticles to be confined to their lowest Landau level. Within this approximation, physical properties exhibit scaling, with the scaling variable¹⁸ $[T-T_{c2}(B)]/(TB)^{2/3}$, but this scaling behavior is not specifically associated with a phase transition. Instead, the magnetic field has the effect of introducing a length scale in the plane perpendicular to the field direction which restricts the divergence in the coherence length¹⁵ and removes the singularity in the specific heat.

In principle, critical and LLL scaling cannot hold in the same region of the $B:T$ plane. Regions of the phase diagram where each scaling form might be expected to hold are discussed in Ref. 10. While the quantitative extent of these regions cannot be determined reliably, estimates within the Hartree approximation¹⁰ suggest that the crossover from critical to LLL scaling should occur at fields of the order of 10 T in a high- T_c material such as YBaCuO, but of the order

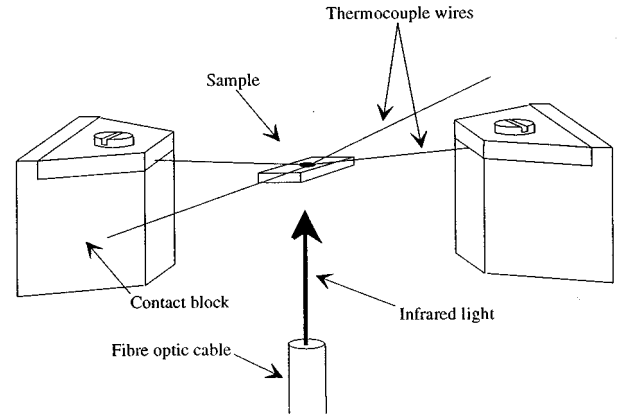


FIG. 1. Experimental arrangement of the single crystals during measurements.

of 10^{-4} T in conventional superconductors such as niobium. Experimentally, however, the two types of scaling may be quite hard to distinguish. Indeed, the scaling expressions for the resistivity and magnetization are similar. Measurements on $\text{YBa}_2\text{Cu}_3\text{O}_{7-\delta}$ seem to be reasonably consistent with both^{5,14,16} and this has led to some controversy.

In this paper, we report measurements of the specific heat of two twinned and one detwinned single-crystal samples of $\text{YBa}_2\text{Cu}_3\text{O}_{7-\delta}$ in magnetic fields up to 8 T, applied parallel to the c axes of the crystals. Resistivity¹⁶ and specific heat¹¹ measurements on one sample (Y8) were reported earlier, and were shown to be consistent with single-parameter critical scaling (for fields up to 4 T in the case of resistivity and 8 T in the case of specific heat) over a temperature range of 10 K above and below T_c .

EXPERIMENTAL DETAILS

Sample Y8 was grown in Leeds using a self-flux technique in an yttria-stabilized zirconia crucible. It was annealed in dry flowing oxygen (at 1 atm) for 14 days at 400, 450, and 500 °C. Measurements of the resistivity were performed after each anneal and the specific heat was measured after the final anneal. Sample A27a1 was grown in Oxford using a self-flux technique in a yttria crucible. Sample A27a1 received no annealing before the specific-heat measurements. Sample DT3c was grown (and detwinned) in Birmingham using a self-flux technique in a zirconia crucible. After growth the sample was annealed at 450 °C for 24 h at a pressure of 145 bar (85 bar at room temperature). The sample was then detwinned by applying uniaxial stress of 50 MPa, the stress was applied at 100 °C, and the crystal was then heated and was completely detwinned at a temperature of 350 °C. Sample DT3c was then annealed for 37 days at 400 °C in flowing oxygen.

The specific heat was measured using an ac technique similar to the method used by Salamon *et al.*² The samples were mounted on crossed thermocouple junctions made by spot welding 25 μm chromel and constantan wires into the arrangement shown in Fig. 1. The samples were physically and thermally attached to the thermocouple junctions using a thin veneer of GE varnish. The heating of the sample was achieved using an infrared LED attached to a fiber-optic

cable. The LED remained outside the cryostat and the fiber-optic cable was fed down the sample probe. The end of the fiber was held approximately 5 mm behind the sample and this distance was adjusted so that the diverging light beam covered the whole crystal and provided homogeneous heating. The output power of the LED was varied sinusoidally in time with a frequency of 17 Hz and the amplitude of the power oscillations was chosen to produce temperature oscillations of approximately 15 mK. At this frequency the magnitude of the temperature oscillations is inversely proportional to the specific heat of the sample. The sample space contains ^4He gas at a pressure of 0.5 atm which provides the thermal link between the sample and a platinum thermometer embedded in a copper block. Because the sample is being heated by the LED the sample temperature is slightly higher than the thermometer temperature and this dc temperature difference was measured on the second arm of the thermocouple. Although this technique is ideal for making very sensitive measurements at a fine temperature resolution the measured signal is proportional to the specific heat within an unknown normalization factor, therefore we normalize our data using published values for the specific heat of $\text{YBa}_2\text{Cu}_3\text{O}_{7-\delta}$ at 100 K. This technique allows the specific heat to be measured with a sensitivity of 1 part in 10^4 with a temperature resolution of 15 mK.

THEORETICAL CONSIDERATIONS

In the critical scaling region, if $\alpha < 0$, the fluctuation specific heat is predicted to have the form¹⁰

$$C_f = C_0 - B^{|\alpha|/2\nu} f(t_B/B^{1/2\nu}), \quad (1)$$

where

$$t_B = \frac{T - T_c(B)}{T_c(B)}. \quad (2)$$

We note that for extreme type-II superconductors $B \approx \mu_0 H$, where H is the applied field, so B and H are to a large extent interchangeable. For the rest of this paper we will use B to denote the magnetic field and the units of B will be T.

In an applied magnetic field there is no feature with which to associate with $T_c(B)$ so we take $T_c(B)$ to be given by

$$T_c(B) = T_c(0) + \frac{dT_c}{dB} B. \quad (3)$$

Some workers use the inflection point on the high-temperature side of the transition to define $T_c(B)$ but there is no real theoretical justification for this. In conventional superconductors^{18,21} we find B_{C2} is a point on the high-temperature side of the inflection point; a point chosen to give good LLL scaling. So as to be consistent with conventional superconductors, for each sample, we estimate a fixed value of dT_c/dB so that the line $T_c(B)$ lies just above the inflection point. The specific heat therefore has a cusp of height C_0 at $t_B = 0$ and $B = 0$. The value of the critical exponent $\alpha = 2 - d\nu$ (for a system of spatial dimensionality d) is estimated theoretically⁶ for $d = 3$ as -0.007 ± 0.006 , while its measured value¹² for ^4He is -0.013 ± 0.003 . The exact form of the scaling function $f(x)$ is unknown, but its behavior for special values of $x = t_B/B^{1/2\nu}$ can be deduced. With the tem-

perature fixed at its critical value ($T = T_c$ or $t_B = 0$), the only singularity in C_f is at $B = 0$, so we must have

$$C_f = C_0 - f_0 B^{|\alpha|/2\nu}, \quad (4)$$

where $f_0 = f(0)$ is a constant. In the limit of zero field ($t_B = t$), on the other hand, the scaling function should behave as $f(x) \approx A^\pm (|x|)^{|\alpha|}$, where the upper (lower) sign refers to $t > 0$ ($t < 0$), so that

$$C_f = \begin{cases} C_0 - A^+ t^{|\alpha|} & (t > 0), \\ C_0 - A^- (-t)^{|\alpha|} & (t < 0). \end{cases} \quad (5)$$

The amplitude ratio $R = A^+/A^-$ is a universal quantity, whose value is estimated theoretically¹⁷ as 1.029 ± 0.013 , while its measured value¹² in liquid ^4He is 1.058 ± 0.004 .

If the fluctuations are assumed to be Gaussian then, for a d -dimensional system, the fluctuation contribution to the specific heat is given by¹

$$C_f = \begin{cases} C^+ t^{-4-d/2} & (t > 0), \\ C^- t^{-4-d/2} + \Delta C_{\text{GL}} & (t < 0), \end{cases} \quad (6)$$

where ΔC_{GL} is the Ginzburg-Landau mean-field specific heat below T_c . This is given by¹⁸

$$\Delta C_{\text{GL}} = T \frac{\alpha'^2}{\beta}, \quad (7)$$

where α and β are the usual Ginzburg-Landau free-energy expansion coefficients (α' is the temperature derivative of α). To a first approximation α' and β are constant but this is only true close to $T_c(B)$. When considering temperatures away from $T_c(B)$ we must account for the temperature dependence of α' and β . The detailed temperature dependence of α' and β is not known so we expand ΔC_{GL} for small t about $t = 0$, as

$$\Delta C_{\text{GL}}(T) \approx hT(1 + gt). \quad (8)$$

This form of $\Delta C_{\text{GL}}(T)$ is now the same as the BCS mean-field specific heat¹⁹ $\Delta C_{\text{BCS}}(T)$ where

$$\Delta C_{\text{BCS}}(T) \approx \gamma T(1 + dt). \quad (9)$$

It will be seen later that the determination of the mean-field specific heat is important when we come to consider lowest Landau level scaling.

The ratio of the fluctuation amplitudes C^+/C^- contains information about the symmetry of the superconducting order parameter. For a BCS superconductor the pairing is s wave and the order parameter is a single complex number. The number of components of the order parameter in this case is 2. In general, the number of components of the order parameter is not a universal quantity.²⁰ If an effective number of components, n_{eff} , of the order parameter is defined by

$$\frac{n_{\text{eff}}}{2^{3/2}} = \frac{C^+}{C^-} \quad (10)$$

then the value of n_{eff} is dependent on the nature of the superconductivity. Values of $n_{\text{eff}} > 2$ imply unconventional (i.e., non- s -wave) superconductivity. $\text{YBa}_2\text{Cu}_3\text{O}_{7-\delta}$ has orthorhombic symmetry therefore the order parameter is also expected to have orthorhombic symmetry. In this case both

s-wave and *d*-wave pairing have $n_{\text{eff}}=2$. The only order parameter with orthorhombic symmetry and a value of $n_{\text{eff}}>2$ is for triplet *p*-wave pairing and in this case n_{eff} has an upper bound of 6. Strictly speaking $\text{YBa}_2\text{Cu}_3\text{O}_{7-\delta}$ has orthorhombic symmetry but in reality it is only slightly distorted from tetragonality. For tetragonal symmetry values of $n_{\text{eff}}>2$ are found for selected *d*-wave symmetries and in this case n_{eff} has an upper bound of 5.65.

In the presence of a magnetic field the transition temperature of a conventional superconductor is reduced, the height of the specific heat peak is suppressed and the width of the transition is increased. The physical origin of the transition broadening was first proposed by Lee and Shenoy.¹⁵ The central idea is that the presence of a magnetic field introduces a length scale perpendicular to the direction of the magnetic field because the paired quasiparticles occupy Landau orbits. In a sufficiently strong magnetic field the paired quasiparticles are confined to the lowest Landau level (LLL) and the dimensionality of the superconductor is reduced by 2. Thus a three-dimensional superconductor becomes equivalent to a collection of one-dimensional filaments and this reduction in dimensionality increases the effect of thermodynamic fluctuations. In this case it is possible that mean-field theory with Gaussian corrections is an appropriate description for zero magnetic field but in the presence of a magnetic field the fluctuations are so enhanced that we need to consider higher-order terms in the Ginzburg-Landau free-energy expansion. Theoretically the problem is difficult for an arbitrary magnetic field because of the need to perform summations over all occupied Landau levels. The problem is much simplified by assuming that the applied magnetic field is large enough to confine the paired quasiparticles to the lowest Landau level. Using a Hartree approximation and assuming that the electrons are confined to the lowest Landau level the fluctuation contribution to the specific heat [$C_f(B, T)$] of a superconductor is predicted to scale as¹⁸

$$\frac{C_f(B, T)}{\Delta C_{\text{GL}}(B, T)} = L\left(\frac{T - T_c(B)}{(TB)^{2/3}}\right), \quad (11)$$

where $L(x)$ is the LLL scaling function. It is now apparent that in order to test LLL scaling we must have a reliable estimate of $\Delta C_{\text{GL}}(B, T)$. Farrant and Gough²¹ have analyzed the specific heat of Niobium which clearly shows LLL scaling. In their analysis they measure the specific heat well below $T_c(B)$, which should be a good estimate of the mean-field specific heat, and then extrapolate this linearly into the transition region. This method does, in principle, give a reliable estimate of the mean-field specific heat [see Refs. 22 and 23 for a discussion of the correct form of $\Delta C_{\text{GL}}(B, T)$]. Some workers have looked for LLL scaling.²⁴⁻³⁰ Welp *et al.*¹⁴ and Janod *et al.*²⁸ do not find clear evidence for LLL scaling. Kobayashi *et al.*²⁹ seemed to find evidence for LLL scaling in BiSCCO but only over a very small range of t_B and only then after using an unusual variation of $T_c(B)$. Zhou *et al.*²⁷ claimed to have found LLL scaling in the specific heat of LuBaCuO, but we believe that, while in the highest field LLL seems to work, the data are better described by the 3D *X*–*Y* model in the field range below about 8 T, as we show below. Recently Roulin *et al.*³⁰ have tried to look for scaling in the field and temperature derivative of the

specific heat in an attempt to remove the difficulties of the background subtraction. They find that their data can be scaled by both LLL and 3D *XY* models. Much of this is also discussed in a recent review by Junod.³¹

In addition to the fluctuation contribution C_f , the measured total specific heat C_{tot} includes nonsingular phonon and normal-electron contributions C_{ns} . These contributions exhibit no sharp features near T_c . Therefore in the following analysis we take the total specific heat to be $C_{\text{tot}} = C_{\text{ns}} + C_f$, with a nonsingular contribution of the form $C_{\text{ns}} = at^2 + bt + c$ where a , b , and c are constants. Because we only consider the specific heat over a 20 K temperature range around T_c we believe that this form of C_{ns} can correctly account for the nonsingular contributions. Some workers²⁴ measure the specific heat over a large temperature range, exclude the region around T_c and then fit the remaining data to more complex models of the phonon specific heat. This method therefore assumes a particular form for the nonsingular contributions. We assume only that nonsingular contributions vary smoothly with temperature for the small temperature range of interest around T_c . A recent criticism of the critical fluctuation model concerns the entropy associated with the superconducting fluctuations. Schnelle *et al.*²⁵ claim that there is too much entropy associated with the fluctuations. The entropy S_f associated with the fluctuations can be calculated from the specific heat using the thermodynamic relation

$$S_f = \int \frac{C_f}{T} dT. \quad (12)$$

Therefore in order to calculate the entropy S_f we need to know C_f . From an analysis of the data using the 3D *X*–*Y* model the fluctuation contribution to the specific heat cannot be separated from the nonsingular contribution because the parameter c is not uniquely defined. Fits to the data give a value only for $(C_0 + c)$. This is not a problem for an analysis based on the Gaussian fluctuation model. But for the critical region, because α is small, the cusp is very close to a logarithmic divergence and experimentally it is impossible to distinguish between the two. In the limit of small α the fluctuation contribution to the specific heat can thus be approximated by²⁵

$$C_f = A \ln(t). \quad (13)$$

Schnelle *et al.*²⁵ used this form for C_f but strictly speaking this is incorrect. Equation (13) gives the singular temperature dependence of C_f not the total value of C_f . The total fluctuation contribution to the specific heat is given by

$$C_f = A \ln(t) + B. \quad (14)$$

Therefore curve fits with this model, including a smooth polynomial background ($at^2 + bt + c$) will give a value ($c + B$) and not a value of c alone. The background specific heat, and therefore C_f , will be unknown to within an additive constant. It is therefore apparent that the entropy associated with the fluctuations cannot be reliably estimated from the zero-field curve fits to the specific heat when using the critical fluctuation model, unless some way of finding the height of the cusp can be found.

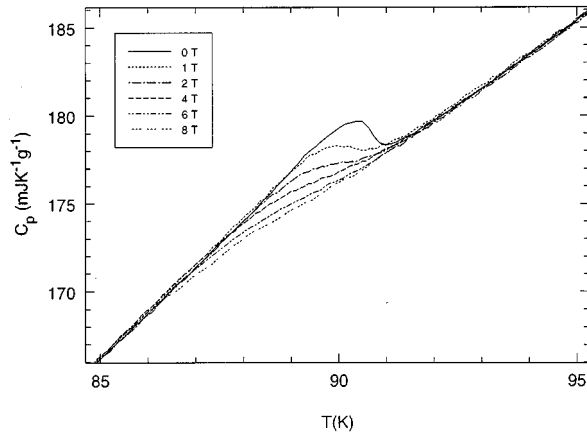


FIG. 2. The specific heat of sample DT3c in magnetic fields of 0, 1, 2, 4, 6, and 8 T (from top to bottom) as indicated in the legend.

RESULTS AND DISCUSSION

Figures 2 and 3 show the specific heat of samples DT3c and A27a1. The size of the jump is similar for all the samples ($\sim 2\%$ of the total specific heat) and all the transitions are around 90 K. The approximate zero-field transition widths are 0.3 K (Y8), 1.0 K (DT3c), and 1.5 K (A27a1), and do not correlate with the T_c 's.

We fit the zero-field data to the 2D and 3D Gaussian models and the 3D $X-Y$ model. In performing the fits we excluded data close to the peak so as to minimize the effects of intrinsic broadening. We therefore ignored data in a region of 2 K for DT3c and A27a1, and 0.6 K for Y8 centered on the peak temperature. We then fixed the value of T_c , slightly above the inflection point on the high temperature side of the transition, and performed a least-squares fit over a reduced temperature range $-0.1 \leq t \leq 0.1$. When performing the Gaussian fits we initially used seven free fitting parameters, a , b , and c for the background specific heat; h and g for the mean-field specific heat, and C^+ and C^- for the fluctuation specific heat. By adjusting all seven parameters, we obtained good fits to the data but the values of the parameters were unphysical. In particular we always obtained $g \sim 10$, which is far too large. In fact a value of $g > 10$ causes $(1 + gt)$ to change sign for $t < -0.1$. In addition to this, the

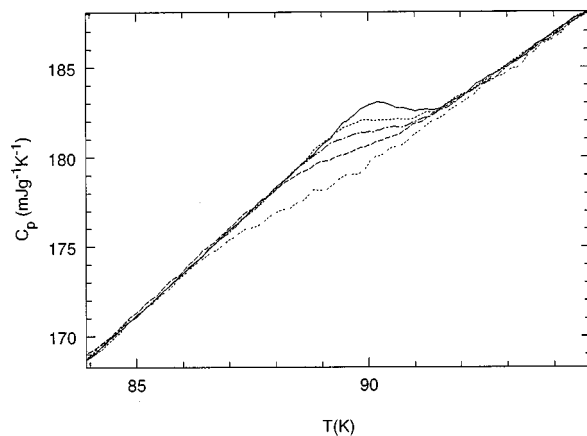


FIG. 3. The specific heat of sample A27a1 in magnetic fields of 0, 1, 2, 4, 6, and 8 T (from top to bottom, see Fig. 2 for the legend).

TABLE I. Parameters derived from the 2D and 3D Gaussian fits to the zero-field specific heat of the three samples. See text for definition of symbols.

Sample	2D Gaussian			3D Gaussian	
	n_{eff}	h ($\text{mJ g}^{-1} \text{K}^{-1}$)	T_c (K)	n_{eff}	h ($\text{mJ g}^{-1} \text{K}^{-1}$)
Y8	2.59	38.5	92.0	2.41	38.7
DT3c	1.79	34.0	90.5	1.63	37.7
A27a	3.09	42.9	90.8	1.82	39.9

value of n_{eff} calculated from Eq. (6) varied from 1.4 to 15.4 depending on the sample. In order to correct this problem we fixed $g=3$ which is a physically reasonable value. The BCS theory predicts $g=1.83$ in the weak-coupling limit, but g is larger for strongly coupled conventional superconductors. The following conclusions are not altered if g is varied in the range $1 < g < 4$ but all the Gaussian curve fits presented here have been calculated with $g=3$. The results of the 2D and 3D Gaussian fits are shown in Table I. Figures 4 and 5 show the results of the 2D and 3D Gaussian fits respectively to the DT3c data. From these figures it is seen that both the 3D and 2D Gaussian models produce reasonable fits to the data although the 3D fit is better than the 2D fit. This is also true for the other samples. The value of n_{eff} calculated from Eq. (10) for each sample varied from 1.6 to 2.4 for the 2D fit and 1.8 to 3.1 for the 3D fit. This large spread in n_{eff} suggests that the Gaussian fluctuation model does not provide a consistent explanation of the fluctuation specific heat. It is important to note that if we fixed $n_{\text{eff}}=2$ we could no longer obtain reasonable fits to the data on any sample.

We now consider the 3D $X-Y$ fit to the zero-field data. We use a , b , c , A^+ , and A^- as free-fitting parameters and fixed $\alpha = -0.013$. Fits of similar quality could be obtained for a wide range of values of α , so we chose to fix the value of α to that obtained in liquid ^4He . We also obtained fits of similar quality using a logarithmic divergence instead of the cusp. Table II shows the parameters found for the best 3D XY fit to each sample and the associated amplitude ratio for each case, and Fig. 6 shows the 3D $X-Y$ fit for sample DT3c, similar to sample Y8 in Ref. 11. Fits to the data on the

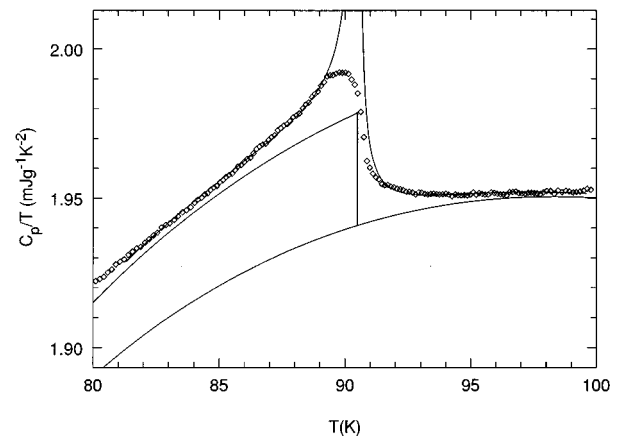


FIG. 4. Specific heat of sample DT3c (points). The solid line is a fit to the data using the 2D Gaussian model with the parameters in Table I. Not all points are shown for clarity.

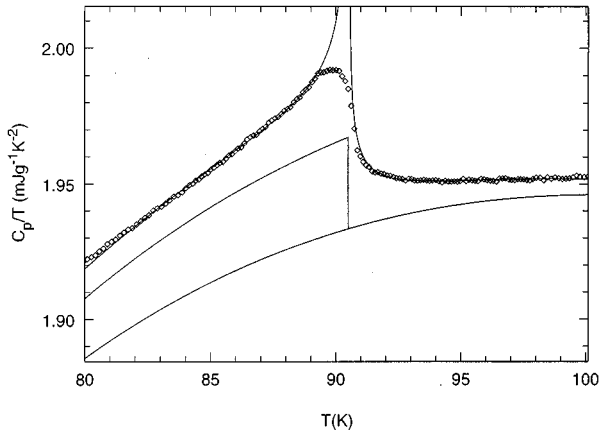


FIG. 5. Specific heat of sample DT3c (points). The solid line is a fit to the data using the 3D Gaussian model with the parameters in Table I. Not all points are shown for clarity.

other samples were of the same quality. The amplitude ratio in all cases is found to be similar to that found in liquid ^4He (1.058). In Fig. 7 we show the specific heat minus the background determined from the 3D XY zero-field fit—in this case the background necessarily includes the height of the cusp, since it is impossible to separate the height of the cusp and the constant in the polynomial background—as a $\log_{10}(|t|)$ plot from which we can see that the fit is reasonable close to T_c from about 5 K above and below T_c , also shown are the lines $A^\pm |t|^\alpha$ from the zero-field fit. From all this we conclude that the 3D X – Y model provides a consistent description of the zero-field specific heat of $\text{YBa}_2\text{Cu}_3\text{O}_{7-\delta}$. The 3D X – Y and 3D Gaussian fits are of similar quality and from the zero-field data it is therefore impossible to distinguish clearly between the critical and Gaussian models although the data is better described by assuming that the fluctuations are three-dimensional.

We now turn to the magnetic field dependence of the specific heat. The specific heats of all our samples have been measured as functions of temperature in constant magnetic fields up to 8 T, applied parallel to the c axis of the crystals. In all cases the transitions display the familiar broadening

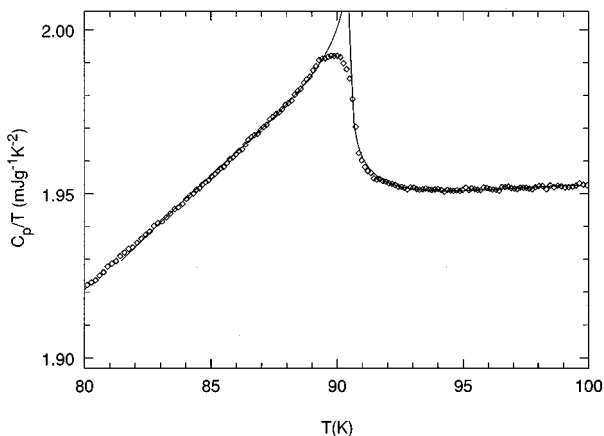


FIG. 6. Specific heat of sample DT3c (points). The solid line is a fit to the data using the 3D X – Y model with the parameters in Table II. Not all points are shown for clarity.

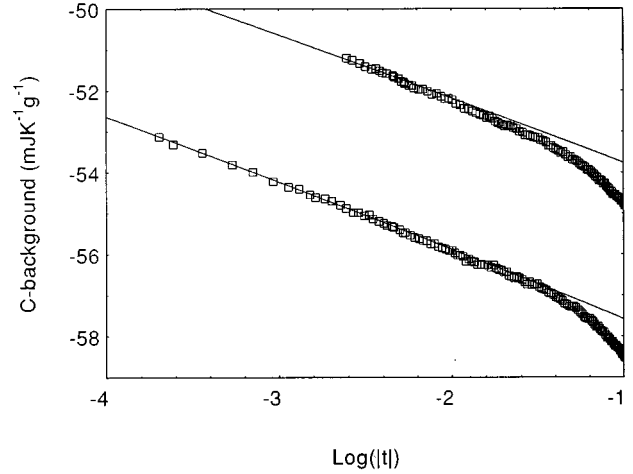


FIG. 7. The specific heat minus the background which includes the height of the cusp C_0 for DT3c plotted vs $\log_{10}(|t|)$. The solid lines are the fits $A^\pm |t|^\alpha$ from the fit in the 3D XY fit. The upper line is for data below T_c and the lower line for data above T_c .

and suppression of the peak with little change in the onset temperature. In all cases the specific heat is field independent (*within* experimental resolution) at temperatures well above and well below the transition temperature from the field and temperature range studied. Figures 2 and 3 show the transitions of samples DT3c and A27a1, respectively, in magnetic fields up to 8 T. The data for sample Y8 are shown in Ref. 11.

We first consider the LLL scaling of the fluctuation specific heat. For a LLL scaling plot the background must come from a Gaussian fluctuation fit in order to be consistent. Because the 3D Gaussian fit is better than the 2D Gaussian fit we use the background obtained from the 3D Gaussian fit. We use a field-independent mean-field specific heat as the normalization factor for the LLL scaling. The mean-field specific heat is in general field dependent, but, as the measured specific heats in different magnetic fields lie close to a common curve well below the transition, it is reasonable to use a field-independent mean-field specific heat. In fact well below T_c there is a small field dependence consistent with entropy balancing. The fluctuation contribution to the specific heat (as defined by the 3D Gaussian fit) is significant at temperatures well below T_c so we do not follow the procedure of Farrant and Gough (i.e., extrapolating the measured specific heat). Instead, we use the mean-field specific heat defined by the 3D Gaussian fit using the parameters in Table I. We note that we arbitrarily set $g = 3$ in Eq. (8) before the fit. We reach the same conclusions if we use any other rea-

TABLE II. Parameters derived from the 3D X – Y fit to the zero-field specific heat of the three samples. See text for definition of symbols.

Sample	T_c (K)	A^+/A^-
Y8	92.0	1.07
DT3c	90.5	1.06
A27a	90.8	1.08

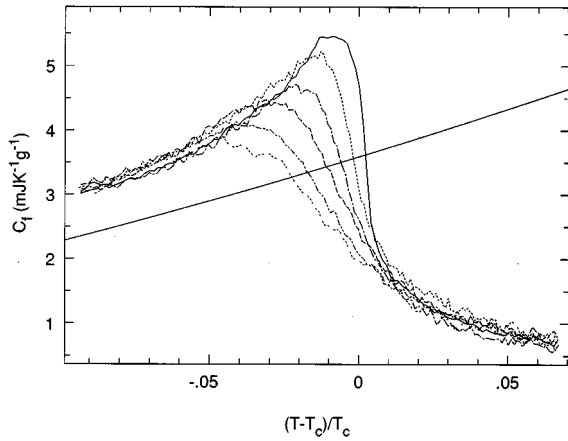


FIG. 8. The fluctuation specific heat of sample DT3c as defined from the zero-field 3D Gaussian fit. The solid line is the mean-field contribution to the specific heat, see Fig. 2 for the legend.

sonable value for g ($1 < g < 4$) or by following the procedure of Farrant and Gough.

The fluctuation specific heat of sample DT3c is shown in Fig. 8, where the solid line is the mean-field specific heat used in the LLL scaling. Figure 9 shows the LLL scaling of the fluctuation specific heat of this sample, using $dT_c/dB = -0.17$ K/T. This value is chosen to be consistent with the transition temperature being on the high-temperature side of the inflection point, this was found to be the case for the LLL scaling in niobium. The scaling is not improved by using any other value of dT_c/dB . From this plot it is apparent that the LLL scaling is not perfect. The scaling improves at higher fields, as expected, and the 6 and 8 T data appear to scale but the lower field data do not seem to scale. The LLL scaling shown in Fig. 9 is characteristic of all the samples and the LLL scaling of the specific heat of sample Y8 is shown in Ref. 23.

The 3D X - Y scaling of the specific heat is easier to perform than the LLL scaling because of the absence of a mean-field normalization factor. We simply use the parameters defined by the zero-field fit to subtract the background and look for scaling of the form given in Eq. (1). Figure 10 shows the 3D X - Y scaling of the specific heat of sample

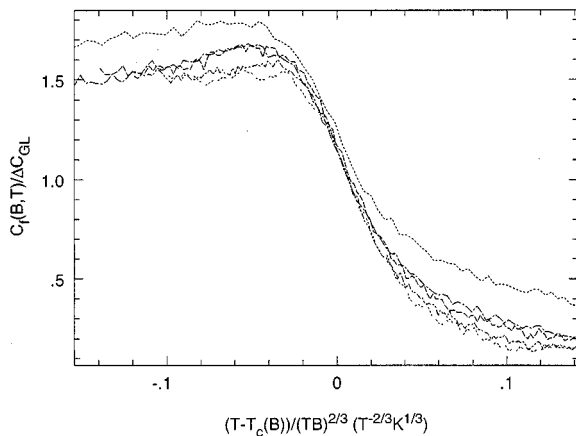


FIG. 9. LLL scaling of the specific heat of sample DT3c, see Fig. 2 for the legend.

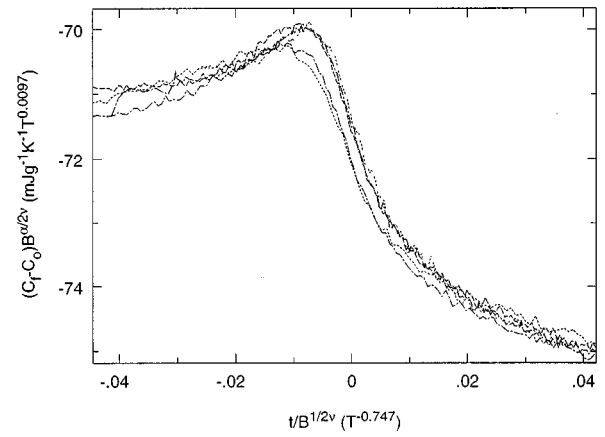


FIG. 10. 3D X - Y scaling of the specific heat of sample DT3c, see Fig. 2 for the legend.

DT3c and Fig. 11 shows the 3D X - Y scaling for sample A27a1. From these scaling plots it is evident that some of the lowest field data do not lie on the scaling curves. We believe this is due to a finite-size effect cutting off the divergence of the coherence length, which is analogous to the effect of a magnetic field. In the presence of finite-size effects critical scaling will only be observed when the characteristic cutoff length due to the applied magnetic field is much shorter than the cutoff length due to the finite-size effect. The failure of the lowest-field data to scale is therefore a reflection on the sample quality not the scaling. We stress here that in this context a finite-size effect is not due to the finite size of the samples. We show below that the cutoff length associated with the finite-size effect is of the order of tens of nanometers and we attribute the finite-size effect to some form of disorder or domain structure on this scale. The finite-size effect will be discussed in more detail below. With the exception of the lowest-field data (because of the finite-size effects) we find that the scaling is excellent for all the samples. The scaling in Figs. 10 and 11 is achieved using t_B as the temperature variable with the values of dT_c/dB shown in Table IV. In fact for $|dT_c/dB| \leq 0.17$ K/T the scaling is insensitive to the exact choice of dT_c/dB . In our original work¹¹ on sample Y8 in fact we implicitly used $dT_c/dB = 0$

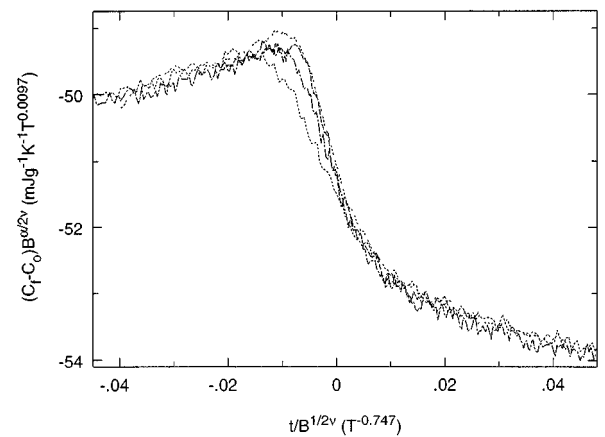


FIG. 11. 3D X - Y scaling of the specific heat of sample A27a1, see Fig. 2 for the legend.

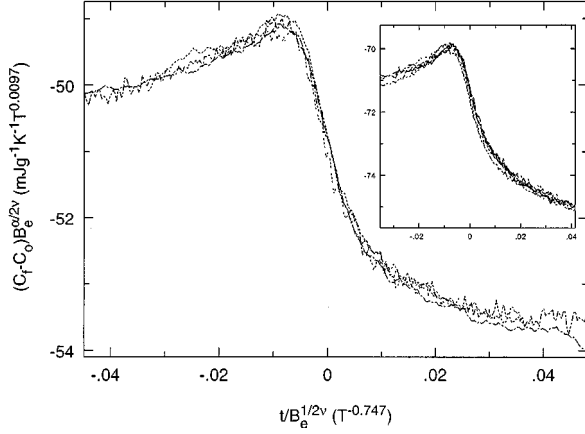


FIG. 12. 3D X – Y scaling of the specific heat of sample A27a1 using the effective magnetic field B_e . Inset: the same plot for sample DT3c, see Fig. 2 for the legend.

but this makes little difference to the scaling. However, we should note that for magnitudes of dT_c/dB bigger than 0.17 K/T the scaling becomes progressively worse. For all the samples studied here we find that 3D X – Y scaling can collapse the data onto a common curve.

We noted previously that the low-field data did not scale. This is the result of a rounding of the transition which maybe due to inhomogeneity but we found we could model it as though it were a finite-size effect. We found that the larger the zero-field transition width, the higher the field needed to observe critical scaling, a fact that is consistent with a finite-size effect. We can model the finite-size effect by following a procedure similar to that of Inderhees *et al.*²⁶ The applied magnetic field B_a introduces a length scale L_B such that

$$L_B = \sqrt{\frac{\hbar}{eB_a}}. \quad (15)$$

Therefore, in analogy, we define a magnetic field B_{FS} equivalent to a finite-size cutoff length L_{FS} as

$$B_{FS} = \frac{\hbar}{eL_{FS}^2}. \quad (16)$$

We then use an effective magnetic field B_e in the scaling Eq. (1) defined as

$$B_e^2 = B_a^2 + B_{FS}^2. \quad (17)$$

This then incorporates the effect of the applied magnetic field and the finite-size effect into the critical scaling. Figure 12 shows the effect of using B_{FS} on the critical scaling of samples A27a1 and DT3c. The shape of the scaling curve is virtually unaffected for the high-field data (as expected) but the low-field data now follow the same curve as the high-field data. The value of B_{FS} needed to scale the low-field data for each sample is shown in Table III (along with the length scale associated with it) and these values correlate well with the zero-field transition widths which implies that the shorter the length scale associated with the finite-size effect the larger the zero-field transition width. Using B_{FS} did not improve the quality of the LLL scaling.

TABLE III. Parameters used in the 3D X – Y scaling. See text for definition of symbols.

3D X – Y scaling parameters				
Sample	$-dT_c/dB$ (K/T)	B_{FS} (T)	ΔT_c (K)	L_{FS} (nm)
Y8	0.17	0.1	0.3	81
DT3c	0.14	0.6	1.0	33
A27a	0.17	1.0	1.5	26

In order to quantify the LLL and 3D XY scaling we evaluated the quantity

$$r = \frac{1}{N_I N_J} \sqrt{\sum_i \sum_j \left(\frac{\bar{y}_i - y_{ij}}{\bar{y}_i} \right)^2},$$

where the y_{ij} are the values of the scaling function evaluated at all magnetic fields indexed by j and all values of the scaling variable. \bar{y}_i are the values of y_{ij} averaged over all magnetic fields (e.g., magnetic fields of 1, 2, 4, 6, 8 T). N_I are the number of data points recorded as the temperature is varied at fixed field and N_J is the number of fixed fields used. The smaller the value of r the better the scaling. For 3D XY scaling using all the data for DT3c $r=0.0016$ while for LLL scaling $r=0.23$ —in both cases we used the best scaling achieved which included the “finite-size scaling” parameter. If we restrict the LLL scaling to field runs of 1, 2, and 4 T then $r=0.18$ and if we restrict the scaling to 6 and 8 T $r=0.048$. These results suggested that 3D XY scaling works well over the whole field range up to 8 T while LLL scaling works best above 6 T.

There has been much debate recently in the literature recently concerning LLL versus critical scaling. Magnetization and resistivity data cannot distinguish between the two scaling regimes. Even with the specific heat there is great difficulty because of the background subtraction problem. The data we have presented suggest that LLL approximation may be valid in magnetic fields greater than about 6 T. Below 6 T the specific heat does not exhibit LLL scaling. The data are also seen to exhibit critical scaling in magnetic fields up to 8 T which suggests that the critical and LLL regimes overlap. Strictly speaking the two regimes cannot overlap because the scaling is of a different kind but the observed overlap is probably due to experimental resolution. If the specific heat was measured in higher magnetic fields then one would expect critical scaling to fail at some large magnetic field although this would be difficult to observe in practice because the specific heat in magnetic fields above 6 T is only weakly field dependent.

The scaling function $f(x)$ has now been determined for three different samples of different quality. In order to compare the scaling functions from different samples we use the general form of the scaling function¹⁰

$$C_f = C_0 - C_1 B^{|\alpha|/2} f_u(x), \quad (18)$$

where $f_u(x)$ is the universal scaling function and C_0 and C_1 are constants which are expected to be sample dependent. The general scaling variable x is defined as

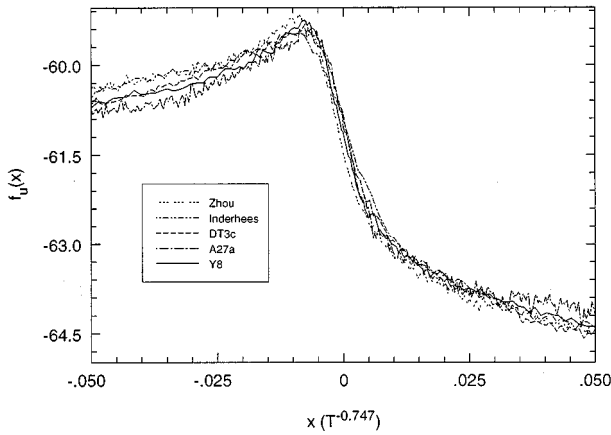


FIG. 13. Experimentally determined scaling functions for Y8, DT3c, A27a, Inderhees' sample, and Zhou's sample plotted together.

$$x = \lambda \frac{t_B}{B^{1/2\nu}}, \quad (19)$$

where λ is a material-dependent constant. λ is expected to have the same value for different samples of $\text{YBa}_2\text{Cu}_3\text{O}_{7-\delta}$ but different values in other materials. The universal scaling function $f_u(x)$ is the same for any superconductor which belongs to the three-dimensional $X-Y$ universality class of the phase transition. We have performed the same analysis on the previously published specific-heat data of Inderhees *et al.*² (a single-crystal sample of $\text{YBa}_2\text{Cu}_3\text{O}_{7-\delta}$) and Zhou *et al.*²⁷ (a single-crystal sample of $\text{LuBa}_2\text{Cu}_3\text{O}_{7-\delta}$). In order to compare the scaling functions from the different samples we take one curve from each scaling plot that is representative of the scaling function and plot these curves in Fig. 13 with the values shown in Table IV. The scaling function is found to be the same, within experimental resolution, for all the samples. In each case the zero-field data are well described by a cusp [Eq. (5)] with an amplitude ratio similar to that found in superfluid ^4He . In each case the specific-heat data in several magnetic fields exhibit single-parameter critical scaling [as described by Eq. (1)] and the scaling functions obtained from the different samples are found to be the same. Whereas C_0 and C_1 are found to be, in general, sample dependent (in some cases they are similar but this may be coincidence) λ is found to be only material dependent (Table IV). To some extent different samples of $\text{YBa}_2\text{Cu}_3\text{O}_{7-\delta}$ are

TABLE IV. The parameters used in Fig. 13. See text for definition of symbols.

Sample	$-dT/dB_{c2}$	C_1	λ
Y8	0.17	1.000	1.00
DT3c	0.17	1.000	1.00
A27a	0.17	1.000	1.00
Inderhees	0.53	0.886	1.00
Zhou	0.33	0.649	0.50

different materials (i.e., different T_c 's, κ 's, etc.) but the properties are expected to be similar. Therefore the fact that the scaling function is the same for different $\text{YBa}_2\text{Cu}_3\text{O}_{7-\delta}$ samples is only a weak test of universality but the fact that the same scaling function is found for the specific heat of $\text{LuBa}_2\text{Cu}_3\text{O}_{7-\delta}$ is a much stronger test of universality. The observed universality of the scaling function is extremely strong evidence that $\text{YBa}_2\text{Cu}_3\text{O}_{7-\delta}$ and $\text{LuBa}_2\text{Cu}_3\text{O}_{7-\delta}$ belong to the three-dimensional $X-Y$ universality class of phase transition.

In summary, we have demonstrated that the specific heat of YBCO single crystals in magnetic fields up to 8 T is well described by the three-dimensional $X-Y$ model. The zero-field specific heat is found to be well described by a cusplike behavior. The specific heat in magnetic fields up to 8 T is found to exhibit critical scaling with the same critical exponents as found in liquid ^4He . Also, we have demonstrated the universality of the critical scaling by comparing the scaling functions obtained in different samples of $\text{YBa}_2\text{Cu}_3\text{O}_{7-\delta}$ and $\text{LuBa}_2\text{Cu}_3\text{O}_{7-\delta}$, the scaling functions are found to be identical within experimental uncertainty. It is still difficult to distinguish between 3D XY and LLL scaling but the demonstration that the scaling curve for different samples in Fig. 13 adds an additional contribution to the debate. We believe our data suggest 3D XY scaling is appropriate at low fields and there maybe a crossover to LLL scaling at higher fields. The crossover field for the samples studied here is about 6 T.

ACKNOWLEDGMENTS

We would like to thank C. C. Huang for permission to use the specific-heat data on $\text{LuBa}_2\text{Cu}_3\text{O}_{7-\delta}$. We would also like to thank the National Crystal Growth Facility at the Universities of Birmingham and Oxford for supplying us with samples. The work was supported by EPSRC in the UK and by NSF DMR91-20000 in the USA.

¹W. J. Skocpol and M. Tinkham, Rep. Prog. Phys. **38**, 1049 (1975).

²M. B. Salamon, S. E. Inderhees, J. P. Rice, B. G. Pazol, D. M. Ginsberg, and N. Goldenfeld, Phys. Rev. B **38**, 885 (1988); S. E. Regan, A. J. Lowe, and M. A. Howson, J. Phys. Condens. Matter **3**, 9245 (1991).

³D. S. Fisher, M. P. A. Fisher, and D. A. Huse, Phys. Rev. B **43**, 130 (1991).

⁴S. Kamal, D. Bonn, N. Goldenfeld, P. Hirschfield, R. Liang, and W. Hardy, Phys. Rev. Lett. **73**, 1845 (1994).

⁵M. B. Salamon, J. Shi, N. Overend, and M. A. Howson, Phys. Rev. B **47**, 5520 (1993).

⁶J. C. Guillou and J. Zinn-Justin, Phys. Rev. B **21**, 3976 (1980).

⁷B. I. Halperin, T. C. Lubensky, and S. K. Ma, Phys. Rev. Lett. **32**, 292 (1974); I. D. Lawrie, Nucl. Phys. B **200**, 1 (1982).

⁸I. D. Lawrie and C. Athorne, J. Phys. A **16**, L587 (1983).

⁹C. Dasgupta and B. I. Halperin, Phys. Rev. Lett. **47**, 1556 (1981).

¹⁰I. D. Lawrie, Phys. Rev. B **50**, 9456 (1994).

¹¹N. Overend, M. A. Howson, and I. D. Lawrie, Phys. Rev. Lett. **72**, 3238 (1994).

- ¹²J. A. Lipa and T. C. P. Chui, *Phys. Rev. Lett.* **51**, 2291 (1983).
- ¹³S. Ullah and A. T. Dorsey, *Phys. Rev. B* **44**, 262 (1991); N. K. Wilkin and M. A. Moore, *ibid.* **48**, 3464 (1993).
- ¹⁴U. Welp, S. Fleshler, K. W. Kwok, R. A. Klemm, V. M. Vinokur, J. Downey, B. Veal, and G. W. Crabtree, *Phys. Rev. Lett.* **67**, 3180 (1991).
- ¹⁵P. A. Lee and S. R. Shenoy, *Phys. Rev. Lett.* **28**, 1025 (1972).
- ¹⁶M. A. Howson, N. Overend, I. D. Lawrie, and M. B. Salamon, *Phys. Rev. B* **51**, 11 984 (1995).
- ¹⁷J. Zinn-Justin, *Quantum Field Theory and Critical Phenomena* (Oxford University Press, Oxford, 1989), p. 623.
- ¹⁸A. J. Bray, *Phys. Rev. B* **9**, 4752 (1974); D. J. Thouless, *Phys. Rev. Lett.* **34**, 946 (1975).
- ¹⁹M. Tinkham, *Introduction to Superconductivity* (Krieger, Malabar, 1980); A. Abrikosov *et al.*, *Methods of Quantum Field Theory in Statistical Physics* (Dover, New York, 1975).
- ²⁰J. F. Annett, M. R. Randeria, and S. R. Renn, *Phys. Rev. B* **38**, 4660 (1988).
- ²¹S. P. Farrant and C. E. Gough, *Phys. Rev. Lett.* **34**, 943 (1975).
- ²²M. A. Howson, N. Overend, and I. D. Lawrie, *Phys. Rev. Lett.* **74**, 1888 (1995).
- ²³S. W. Pierson, J. Buan, B. Zhou, C. C. Huang, and O. T. Valls, *Phys. Rev. Lett.* **74**, 1887 (1995).
- ²⁴A. Junod, E. Bonjour, R. Calemczuk, J. Y. Henry, J. Muller, G. Triscone, and J. C. Vallier, *Physica C* **211**, 304 (1993).
- ²⁵W. Schnelle, P. Ernst, and D. Wohlleben, *Ann. Phys. (Germany)* **2**, 109 (1993).
- ²⁶S. E. Inderhees, M. B. Salamon, J. P. Rice, and D. M. Ginsberg, *Phys. Rev. Lett.* **66**, 232 (1991).
- ²⁷B. Zhou, J. Buan, Stephen Pierson, C. C. Huang, Oriol T. Valls, J. Z. Liu, and R. N. Shelton, *Phys. Rev. B* **47**, 11 631 (1993).
- ²⁸A. Janod, A. Junod, K. Q. Wang, G. Triscone, R. Calemczuk, and J. Y. Henry, *Physica C* **211**, 304 (1993).
- ²⁹N. Kobayashi, K. Egawa, K. Miyoshi, H. Iwasaki, H. Ikeda, and R. Yoshizaki, *Physica C* **219**, 265 (1994).
- ³⁰M. Roulin, A. Junod, and E. Walker, *Physica C* **260**, 259 (1996).
- ³¹A. Junod, in *Studies of High Temperature Superconductors*, edited by A. V. Narlikar (Nova Science, Commack, NY, in press), Vol. 19, p. 1.